Thermodynamic Properties of Dimethyl Carbonate*

Yong Zhou (周永) and Jiangtao Wu (吴江涛)[a)]

MOE Key Laboratory of Thermo-Fluid Science and Engineering, Xi'an Jiaotong University, Xi'an Shaanxi 710049, People's Republic of China

Eric W. Lemmon

Thermophysical Properties Division, National Institute of Standards and Technology, 325 Broadway, Boulder, Colorado 80305, USA

(Received 2 November 2009; accepted 25 October 2011; published online 30 December 2011)

A thermodynamic property formulation for dimethyl carbonate has been developed with the use of available experimental thermodynamic property data. The equation of state was developed with multiproperty fitting methods involving pressure-density-temperature ($p\rho T$), heat capacity, vapor pressure, and saturated-liquid density data. The equation of state conforms to the Maxwell criterion for two-phase liquid-vapor equilibrium states, and is valid for temperatures from the triple-point temperature (277.06 ± 0.63) K to 600 K, for pressures up to 60 MPa, and for densities up to 12.12 mol dm^{-3}. The extrapolation behavior of the equation of state at low and high temperatures and pressures is reasonable. The uncertainties ($k = 2$, indicating a 95% confidence level) of the equation of state in density are 0.05% for saturated-liquid states below 350 K, rising to 0.1% in the single phase between 278 K and 400 K at pressures up to 60 MPa. Due to the lack of reliable data outside this region, the estimated uncertainties increase to 0.5% to 1% in the vapor and critical regions. The uncertainties in vapor pressure are 0.6% from 310 K to 400 K, and increase to 1% at higher temperatures and to 2% at lower temperatures due to a lack of experimental data. The uncertainty in isobaric heat capacity and speed of sound in the liquid phase at saturation or atmospheric pressure is 0.5% from 280 K to 335 K. The uncertainties are higher for all properties in the critical region. Detailed comparisons between experimental and calculated data, and an analysis of the equation, have been performed. © *2011 American Institute of Physics*. [doi:10.1063/1.3664084]

Key words: dimethyl carbonate; equation of state; thermodynamic properties.

CONTENTS

List of Tables

List of Figures

a)Author to whom correspondence should be addressed; electronic mail: jtwu@mail.xjtu.edu.cn; Fax: 86-29-82668789.

*Contribution in part of the National Institute of Standards and Technology, not subject to copyright in the U.S.

Nomenclature

c_p = specific isobaric heat capacity
c_v = specific isochoric heat capacity
c_σ = specific saturation heat capacity
$d, l, t, \beta, \zeta, \varepsilon, \eta$ = exponents
e = specific internal energy
f = specific Helmholtz energy
h = specific enthalpy
i = serial number
k_s = isentropic expansion coefficient
k_T = isothermal expansion coefficient
M = molar mass
N = number of data points
n = coefficients
p = pressure
R = molar gas constant
s = specific entropy
T = temperature
v = specific volume
w = sound speed
Z = compressibility factor

Greek Letters

Δ = deviation
α_v = volume expansivity
γ = Gruneisen parameter
δ = reduced density
ϕ = dimensionless Helmholtz energy
ρ = specific density
τ = inverse reduced temperature
ω = acentric factor

Superscripts

o = ideal-gas
r = residual
′ = saturated-liquid state
″ = saturated-vapor state

Subscripts

0 = reference-state property
c = critical
calc = calculated
exp = experimental
l = liquid property
nbp = normal-boiling-point property
tp = triple-point property
v = vapor property
σ = saturation property

1. Introduction

Dimethyl carbonate (DMC, $C_3H_6O_3$, CAS 616-38-6) is a nonirritating and nontoxic chemical. In recent years, researchers have found that dimethyl carbonate can be used as a fuel additive, because it helps to reduce the vapor pressure of fuels, which in turn reduces the emissions to the atmosphere by evaporation.[1] Carbon monoxide and smoke decrease as the carbonate addition increases; additionally, NO_x emissions do not increase as the amount of dimethyl carbonate increases.[2] Dimethyl carbonate is a strong contender to help the refining industry meet the Clean Air Act[3] because dimethyl carbonate has about three times the oxygen content per volume as methyl *tert*-butyl ether. Dimethyl carbonate blends well with octane; it does not separate in a water stream like some alcohols, has low toxicity, and is quickly biodegradable.[4]

Thermodynamic properties of this fluid are very important for simulating, designing, and optimizing the use of dimethyl carbonate in various systems. This work presents an equation of state for dimethyl carbonate based on an extensive collection of experimental data. The fundamental constants and characteristic properties used in this work are summarized in Table 1. Detailed comparisons between experimental and calculated data have been performed. The extrapolation behavior of the equation of state at low and high temperatures and pressures is shown to be reasonable.

2. Critical and Triple-Point Parameters of Dimethyl Carbonate

The critical parameters are among the most important fundamental properties for a fluid, and are a prerequisite for the development of an equation of state, because they are often used as the reducing parameters for the independent properties. The difficulty of determination of the critical parameters can cause considerable differences among reported values. In this work, the critical temperature obtained by Steele

TABLE 1. Fundamental constants and characteristic properties of dimethyl carbonate

Symbol	Quantity	Value
R	Molar gas constant	8.314 472 J mol^{-1} K^{-1}
M	Molar mass	90.0779 g mol^{-1}
T_c	Critical temperature	557 K
p_c	Critical pressure	4908.8 kPa
ρ_c	Critical density	4.0 mol dm^{-3}
T_{tp}	Triple-point temperature	277.06 K
p_{tp}	Triple-point pressure	2.2 kPa
ρ_{tpv}	Vapor density at the triple point	9.68×10^{-4} mol dm^{-3}
ρ_{tpl}	Liquid density at the triple point	12.111 mol dm^{-3}
T_{nbp}	Normal-boiling-point temperature	363.256 K
ρ_{nbpv}	Vapor density at the normal boiling point	0.035 mol dm^{-3}
ρ_{nbpl}	Liquid density at the normal boiling point	10.813 mol dm^{-3}
ω	Acentric factor	0.346
T_0	Reference temperature for ideal-gas properties	298.15 K
p_0	Reference pressure for ideal-gas properties	1 kPa
h_0^o	Reference ideal-gas enthalpy at T_0	26 712.371 J mol^{-1}
s_0^o	Reference ideal-gas entropy at T_0 and p_0	109.66 202 J mol^{-1} K^{-1}

et al.[5,6] was used as the reducing temperature in the equation of state; this value is (557 ± 2) K. As it is difficult to accurately determine the critical density because of the infinite compressibility at the critical point and the difficulty of reaching thermodynamic equilibrium, the critical density was obtained while fitting the equation of state. The value is (4.0 ± 0.1) mol dm^{-3}. The critical pressure was determined once the final equation of state was obtained. This value is a simple calculation of the pressure at the critical temperature and density. The value is (4908.8 ± 50) kPa.

The triple-point temperature measured by Wachter *et al.*[7] is (277.06 ± 0.63) K. The triple-point pressure and density were calculated here from the final equation of state, and are given in Table 1 along with other calculated values from the equation of state. Ding[8] and Biltz *et al.*[9] also measured the triple-point temperature and reported values of (278.2 ± 1) K and (267.554 ± 0.54) K, respectively.

3. Experimental Data

A literature search was performed for the thermodynamic properties of dimethyl carbonate, including sources obtained from the THERMODATA ENGINE[10] database developed by the Thermodynamics Research Center (TRC) of NIST, and the results are listed in Table 2 with the temperatures converted to ITS-90. Data sets with only one to three data points are labeled as "other data sets" in the plots, except those that were important to the development of the equation of state. Although many researchers have studied the thermodynamic properties of dimethyl carbonate, the experimental data are few and scattered. Even worse, their uncertainties are high compared to those of reference fluids and some refrigerants. A literature survey found that there are 81 articles containing experimental $p\rho T$ data, but, unfortunately, there are only four articles[11–14] containing a significant amount of experimental data, and the other articles contain only experimental values near atmospheric pressure. Many of these were made only to verify the purity of the sample; therefore, there are many duplicated experimental data points, and some deviate substantially from other data.

There are only five articles[5,6,15–17] containing experimental vapor-pressure data over a wide range. Similar to the $p\rho T$ data, many documents report only the normal boiling point to test the purity of the sample. The experimental ranges of the five articles mostly overlap, and the experimental data sets deviate significantly from each other.

A good equation of state should be able to represent well the properties related to energy (such as heat capacity and sound speed). For dimethyl carbonate, there are nine publications (77 data points) with isobaric heat capacity values in the liquid phase, with high deviations among the reported experimental values.[8,18–25]

TABLE 2. Experimental data for dimethyl carbonate

Author (year)	Number of data[a]	Temperature range (K)	Pressure range (MPa)	AAD (%)	Bias (%)
Vapor pressure, p_σ					
Harris (1961)[33]	6	278–328	0.002–0.028	1.208	−1.208
Jiang and Zhang (1987)[15]	38	288–371	0.004–0.127	0.626	0.445
Negadi *et al.* (1993)[32]	9	283–373	0.003–0.137	0.581	−0.581
Comelli and Francesconi (1994)[35]	4	298–333	0.007–0.035	1.098	1.098
Steele *et al.* (1997)[5,6]	18 (10)	311–397	0.013–0.27	0.042	0.032
Rodriguez *et al.* (2002)[16]	131	326–411	0.027–0.384	0.718	0.638
Zhang *et al.* (2003)[36]	4	361–363	0.101	3.436	3.436
Shi *et al.* (2005)[37]	5	337–428	0.041–0.566	0.564	0.449
Fukano *et al.* (2006)[38]	5	337–361	0.04–0.093	0.060	−0.037
Li *et al.* (2008)[39]	4	293–373	0.01–0.14	18.862	17.254
Kozlova *et al.* (2008)[17]	16	274–304	0.002–0.01	2.879	2.879

TABLE 2. Experimental data for dimethyl carbonate—Continued

Author (year)	Number of data[a]	Temperature range (K)	Pressure range (MPa)	AAD (%)	Bias (%)
Saturated-liquid density, ρ'					
Steele *et al*. (1997)[5]	5	308–393		0.027	−0.023
Pardo *et al*. (1999)[18]	4 (1)	278–308		0.017	0.009
Lopez *et al*. (2000)[40]	6	278–323		0.017	0.017
Comunas *et al*. (2001)[12]	8	283–353		0.029	−0.029
Lugo *et al*. (2001)[11]	9 (2)	278–353		0.033	0.032
Pardo *et al*. (2001)[20]	4	288–308		0.019	0.019
Rodriguez *et al*. (2001)[41]	4	293–313		0.018	0.015
Pardo *et al*. (2002)[21]	4	288–308		0.014	0.014
Bi *et al*. (2003)[42]	21	282–383		0.047	−0.047
Romano *et al*. (2003)[43]	5	288–313		0.012	−0.012
Pereiro *et al*. (2004)[44]	5	293–313		0.014	0.014
Rivas *et al*. (2004)[45]	7 (1)	288–328		0.008	0.007
Tojo *et al*. (2004)[46]	6	293–318		0.019	0.017
Troncoso *et al*. (2004)[13]	10	283–328		0.027	−0.023
Yang *et al*. (2004)[47]	7	293–343		0.016	−0.016
Pardo *et al*. (2005)[22]	4	288–308		0.019	0.019
Rodriguez *et al*. (2006)[48]	4	293–313		0.012	0.012
Iglesias-Otero *et al*. (2007)[49]	7	293–323		0.016	0.016
Rivas and Iglesias (2007)[50]	5	288–328		0.007	0.006
Rivas and Iglesias (2008)[51]	5	288–328		0.017	−0.003
Mosteiro *et al*. (2009)[52]	5	288–308		0.021	0.021
Saturated-vapor density, ρ''					
Steele *et al*. (1997)[5]	4	540–557		5.023	1.487
Steele *et al*. (1997)[6]	5	540–557		5.472	2.643
pρT					
Comunas *et al*. (2001)[12]	90 (90)	283–353	5–60	0.016	−0.015
Lugo *et al*. (2001)[11]	72 (72)	278–353	1–25	0.033	0.032
Troncoso *et al*. (2004)[13]	80 (80)	283–328	5–40	0.023	−0.021
Ma and Li (2005)[53]	7	293–343	0.101	0.031	−0.031
Shi *et al*. (2005)[37]	5	337–428	0.101	1.486	−1.486
Wisniak *et al*. (2008)[54]	5	293–313	0.101	0.007	−0.006
Meng *et al*. (2009)[14]	45	283–353	0.1–19.6	0.094	−0.088
Sound speed, *w*					
Rodriguez *et al*. (2001)[41]	4	293–313	Sat. liquid	0.109	−0.100
Pardo *et al*. (2002)[21]	4 (2)	288–308	Sat. liquid	0.147	−0.054
Pereiro *et al*. (2004)[44]	5	293–313	Sat. liquid	0.127	−0.087
Mosteiro *et al*. (2009)[52]	5	288–308	Sat. liquid	0.260	−0.220
Saturation heat capacity, c_σ					
Steele *et al*. (1997)[5,6]	13 (9)	300–540		1.653	−1.553
Isobaric heat capacity, c_p					
Pardo *et al*. (1999)[18]	3	288–308	0.101	0.123	0.123
Regueiro (1999)[19]	4	288–308	0.101	0.041	0.015
Pardo *et al*. (2001)[20]	3 (2)	288–308	0.101	0.029	−0.006
Pardo *et al*. (2002)[21]	3	288–308	0.101	0.029	−0.006
Ding (2004)[8]	40	281–320	0.101	0.541	0.490
Pardo *et al*. (2005)[22]	3	288–308	0.101	0.029	−0.006
Valencia *et al*. (2005)[23]	3	288–308	0.101	0.243	−0.243
Comelli *et al*. (2006)[24]	10	288–333	0.101	3.882	−3.882
Comelli *et al*. (2010)[25]	8	288–323	0.101	1.803	1.803

[a]Numbers listed in parentheses are the number of data points used in the fit, although the statistics given in the table include all data.

4. Equation of State

4.1. The formulation of the equation of state

The equation of state is formulated with the Helmholtz energy as the fundamental property, with independent variables of temperature and density. The Helmholtz energy is divided into two parts. One part describes the ideal gas at the given temperature and density, and the other part describes the residual properties of the fluid. This type of equation has the advantage that all thermodynamic properties can be derived simply from the equation of state; more information can be found in the books of Span[26] and Jacobsen *et al.*[27] The Helmholtz energy is represented as

$$f(T,\rho) = f^{o}(T,\rho) + f^{r}(T,\rho), \tag{1}$$

where the superscript o denotes the ideal-gas Helmholtz energy and the superscript r denotes the residual Helmholtz energy. The ideal-gas Helmholtz energy is given by

$$f^{o}(T,\rho) = h^{o}(T) - RT - Ts^{o}(T,\rho). \tag{2}$$

The ideal-gas enthalpy h^{o} is a function only of temperature T, and the ideal-gas entropy s^{o} is a function of temperature T and density ρ. This equation can be expressed as a function of the ideal-gas isobaric heat capacity

$$f^{o}(T,\rho) = \left(\int_{T_0}^{T} c_p^{o}\mathrm{d}T + h_0^{o}\right) - RT - T \times \left[\int_{T_0}^{T} \frac{c_p^{o} - R}{T}\mathrm{d}T - R\ln\left(\frac{\rho}{\rho_0^{o}}\right) + s_0^{o}\right], \tag{3}$$

where $R = 8.314\ 472$ J mol^{-1} K^{-1} is the molar gas constant,[28] and ρ_0^{o}, h_0^{o}, and s_0^{o} are properties at the reference state (T_0, p_0). In this equation, c_p^{o} is the ideal-gas heat capacity as a function of temperature T.

The equation of state used in this work is explicit in the dimensionless Helmholtz energy

$$\phi(\tau,\delta) = \frac{f(T,\rho)}{RT} = \frac{f^{o}(T,\rho)}{RT} + \frac{f^{r}(T,\rho)}{RT} = \phi^{o}(\tau,\delta) + \phi^{r}(\tau,\delta), \tag{4}$$

where the dimensionless ideal-gas Helmholtz energy, derived from Eq. (3), is given by,

$$\phi^{o}(\tau,\delta) = \frac{h_0^{o}\tau}{RT_c} - \frac{s_0^{o}}{R} - 1 + \ln\frac{\delta\tau_0}{\delta_0\tau} - \frac{\tau}{R}\int_{\tau_0}^{\tau}\frac{c_p^{o}}{\tau^2}\mathrm{d}\tau + \frac{1}{R}\int_{\tau_0}^{\tau}\frac{c_p^{o}}{\tau}\mathrm{d}\tau, \tag{5}$$

with inverse reduced temperature $\tau = T_c/T$ and reduced density $\delta = \rho/\rho_c$.

As shown in the above formulation, the dimensionless ideal-gas Helmholtz energy can be derived from the ideal-gas isobaric heat capacity if the reference state is given. In this work, the reference state is defined by setting the enthalpy and entropy of the saturated liquid to zero at the normal boiling point. The ideal-gas isobaric heat capacity formula is

$$\frac{c_p^{o}}{R} = n_0^{o} + \sum_{i=1}^{4} n_i^{o}\left(\frac{t_i^{o}}{T}\right)^2 \frac{\exp(t_i^{o}/T)}{\left[\exp(t_i^{o}/T) - 1\right]^2}, \tag{6}$$

where the coefficients n_i^{o} and exponents t_i^{o} are given in Table 3. These coefficients and exponents were obtained simultaneously with the parameters of the reduced Helmholtz energy during fitting. The functional form in Eq. (6) is superior to a polynomial form in that the extrapolation behavior at high temperatures is consistent with physical models. A more convenient form of the dimensionless ideal-gas Helmholtz energy, derived from the integration of Eq. (5) and the application of the reference state, is

$$\phi^{o}(\tau,\delta) = \ln\delta + \left(n_0^{o} - 1\right)\ln\tau + n_5^{o} + n_6^{o}\tau + \sum_{i=1}^{4} n_i^{o}\ln\left[1 - \exp\left(\frac{-t_i^{o}\tau}{T_c}\right)\right], \tag{7}$$

where the values of the coefficients n_i^{o} and exponents t_i^{o} are the same as those in Eq. (6) and are given in Table 3.

The coefficients and exponents of the residual Helmholtz energy were determined from experimental data, and many constraints were added to the fit to ensure good extrapolation behavior of the equation of state. These constraints have been explained elsewhere by Span and Wagner,[29] Lemmon and Jacobsen,[30] and Lemmon *et al.*[31] In this work, the fitting methods by Lemmon and Jacobsen[30] and Lemmon *et al.*[31] were employed to fit the equation of state. The equation for the residual Helmholtz energy obtained in this work is

$$\phi^{r}(\tau,\delta) = \sum_{i=1}^{6} n_i\delta^{d_i}\tau^{t_i} + \sum_{i=7}^{12} n_i\delta^{d_i}\tau^{t_i}\exp\left(-\delta^{l_i}\right) + \sum_{i=13}^{18} n_i\delta^{d_i}\tau^{t_i}\exp\left(-\eta_i(\delta-\varepsilon_i)^2 - \beta_i(\tau-\zeta_i)^2\right), \tag{8}$$

where the coefficients and exponents obtained in this work are given in Table 4. The equation of state is valid from the triple-point temperature to 600 K, for pressures up to

TABLE 3. Coefficients and exponents of the ideal-gas isobaric heat capacity equation

i	n_i^{o}	t_i^{o}
0	9.284 21	-
1	1.485 25	21
2	0.822 585	1340
3	16.245 3	1672
4	1.159 25	7395
5	4.991 646 2	-
6	−0.170 944 9	-

TABLE 4. Coefficients and exponents of the residual Helmholtz energy equation

i	n_i	t_i	d_i	l_i	η_i	β_i	ζ_i	ε_i
1	0.000 526 831 87	1	5	-	-	-	-	-
2	1.353 396	0.227	1	-	-	-	-	-
3	−2.649 283	1.05	1	-	-	-	-	-
4	−0.278 541 2	1.06	2	-	-	-	-	-
5	0.174 255 4	0.5	3	-	-	-	-	-
6	0.031 606 252	0.78	4	-	-	-	-	-
7	0.399 866	1.3	1	1	-	-	-	-
8	1.178 144	1.347	2	1	-	-	-	-
9	−0.023 528 1	0.706	7	1	-	-	-	-
10	−1.015	2	1	2	-	-	-	-
11	−0.788 043 6	2.5	2	2	-	-	-	-
12	−0.126 96	4.262	3	2	-	-	-	-
13	1.219 8	1	1	-	0.9667	1.240	1.2827	0.6734
14	−0.488 3	2.124	1	-	1.5154	0.821	0.4317	0.9239
15	−0.003 329 3	0.4	2	-	1.0591	15.45	1.1217	0.8636
16	−0.003 538 7	3.5	2	-	1.6642	2.210	1.1871	1.0507
17	−0.511 72	0.5	3	-	12.4856	437.0	1.1243	0.8482
18	−0.168 82	2.7	3	-	0.9662	0.743	0.4203	0.7522

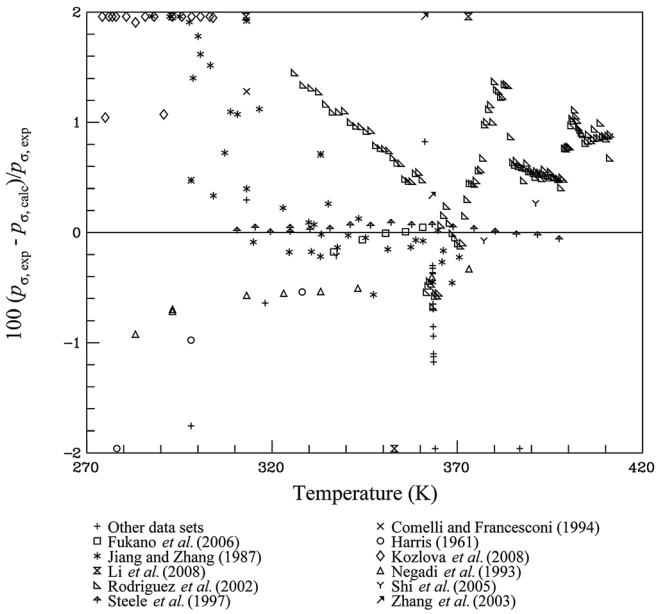

FIG. 1. Comparisons of vapor pressures p_σ calculated with the equation of state to experimental data.

60 MPa, and for densities up to 12.12 mol dm^{-3}. Equations for calculating pressure, enthalpy, entropy, heat capacity, and sound speed can be found in Lemmon *et al.*[31]

4.2. Comparisons with experimental data

The percentage deviation between the experimental data and the values calculated from the equation for any property, X, is defined as

$$\Delta X = 100\left(\frac{X_{\text{exp}} - X_{\text{calc}}}{X_{\text{exp}}}\right). \tag{9}$$

With this definition, the average absolute deviation (AAD) is defined as

$$\text{AAD} = \frac{1}{N_{\text{exp}}}\sum_{i=1}^{N_{\text{exp}}} |\Delta X_i|, \tag{10}$$

where N_{exp} is the number of experimental data points. The Bias is defined as

$$\text{Bias} = \frac{1}{N_{\text{exp}}}\sum_{i=1}^{N_{\text{exp}}} (\Delta X_i). \tag{11}$$

The AAD and Bias between the experimental data and the values calculated from the equation of state are listed in the last two columns of Table 2.

Deviations between experimental data and values calculated with the equation of state are shown in plots, beginning with the vapor pressure in Fig. 1. There are considerable deviations among the vapor-pressure data sets of dimethyl carbonate, and comparisons of experimental vapor pressures with values calculated by the equation of state are presented in Fig. 1. As shown in this figure, most of the deviations are within 1%. The equation represents the data by Steele *et al.*[5,6] generally within 0.2%. There are many normal boiling temperatures reported; the equation represents most of them within 0.6%. At low temperature, the data by Kozlova *et al.*[17] and Jiang and Zhang[15] show positive deviations, whereas the data by Negadi *et al.*[32] and Harris[33] show negative deviations. Additionally, there are no data reported above 430 K.

The equation of state represents experimental saturated-liquid density data to within their uncertainty, which is generally within 0.04%, as shown in Fig. 2. However, these data were measured over a very limited temperature range (from 278 K to 393 K). As the saturated-vapor density data are very few, comparisons of experimental data with values calculated from the equation of state are not shown in the form of a diagram. The only available data by Steele *et al.*[5,6] are close to the critical point.

In the liquid region, deviations between the experimental $p\rho T$ data and the values calculated from the equation of state are within 0.05% to 0.1% between 278 K and 400 K, except for the data by Meng *et al.*[14] that were obtained with a vibrating-wire instrument; these deviations are within 0.2%. Figure 3 shows comparisons of experimental $p\rho T$ data sets with values calculated from the equation of state as a function of pressure. There are no $p\rho T$ data in the vapor phase. We used various constraints to ensure that the properties in the vapor region are represented as well as possible without data. Figure 4, in which the y-intercept (zero density) represents the second virial coefficient at a given temperature, and the third virial coefficient is the slope of each line at zero density, shows that the behavior of the second, third, and

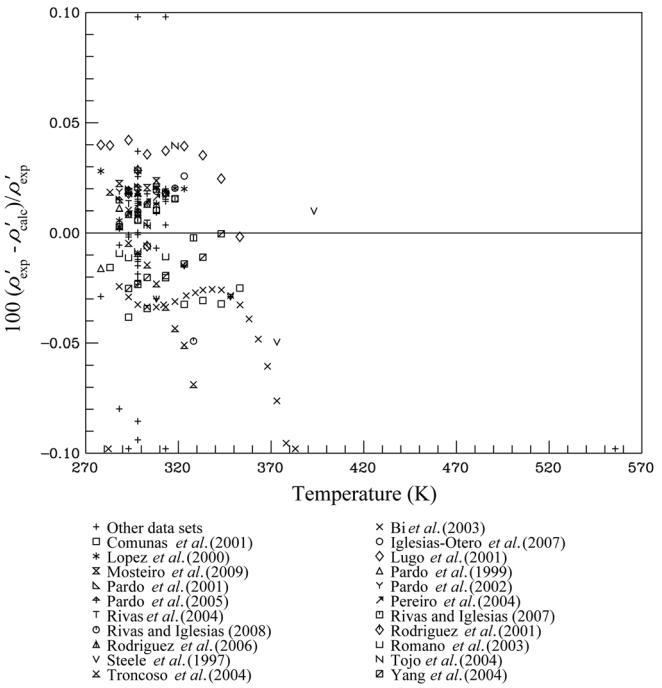

FIG. 2. Comparisons of saturated-liquid densities ρ' calculated with the equation of state to experimental data.

fourth virial coefficients, as well as the shape of the equation of state, are reasonable. These virial coefficients define the behavior in the vapor phase.

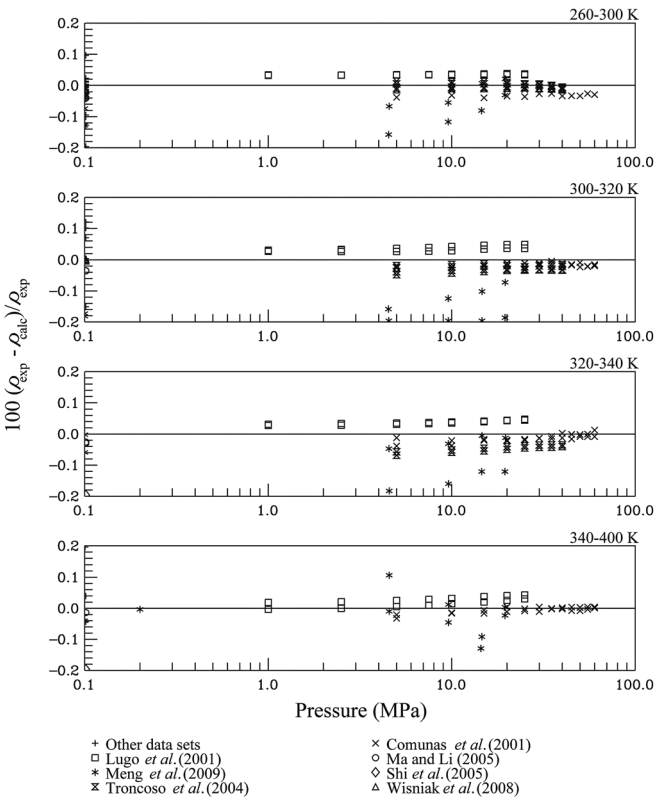

FIG. 3. Comparisons of densities ρ calculated with the equation of state to experimental data.

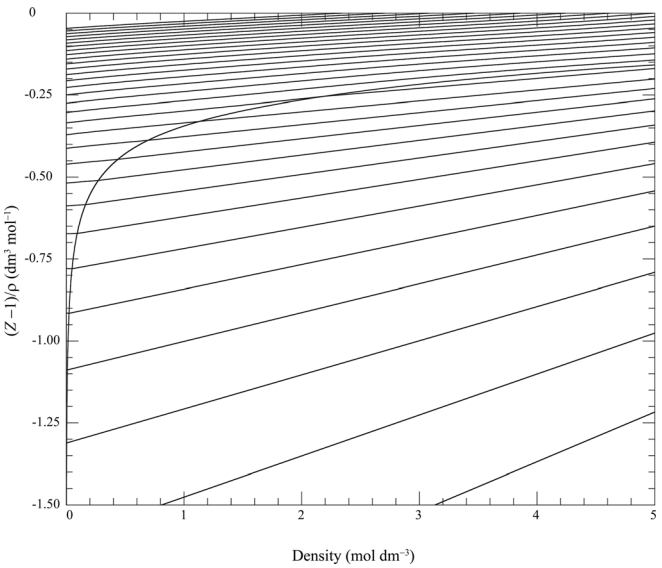

FIG. 4. Calculations of $(Z-1)/\rho$ along isotherms versus density ρ. The intersecting curve is the saturation line. Isotherms are shown at temperatures from 250 to 1000 K with an interval of 25 K.

Comparisons of experimental isobaric heat-capacity data with values calculated from the equation of state are presented in Fig. 5. Deviations between the experimental isobaric heat-capacity data and the values calculated from the equation of state are within 1%, except for the data by Comelli *et al.*,[24,25] who reported two data sets that differ substantially. One has large positive deviations and the other negative deviations. Figure 6 shows comparisons of experimental saturation heat-capacity data with values calculated from the equation of state; the deviations are within 0.5% below 460 K, and there is a downward trend as the data approach the critical point. The sound speed data are very

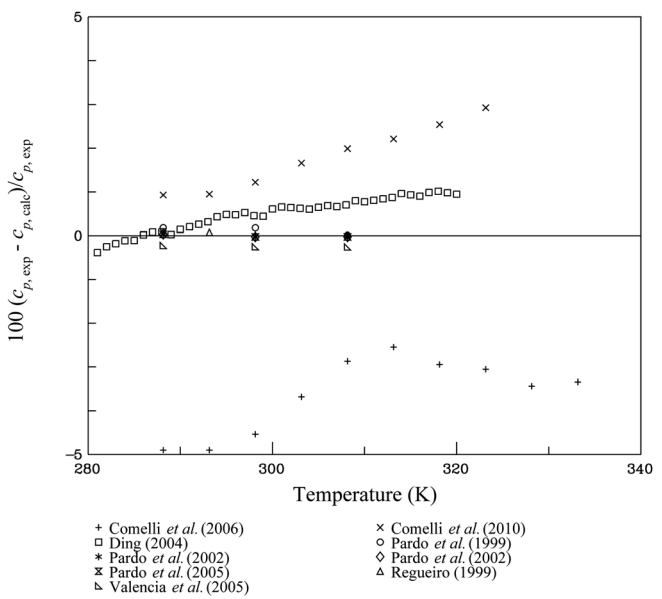

FIG. 5. Comparisons of atmospheric pressure isobaric heat capacities c_p calculated with the equation of state to experimental data.

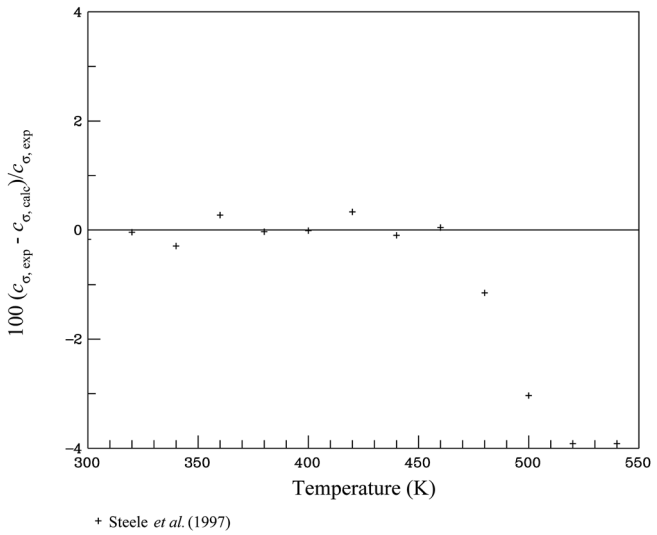

FIG. 6. Comparisons of saturation heat capacities c_σ calculated with the equation of state to experimental data.

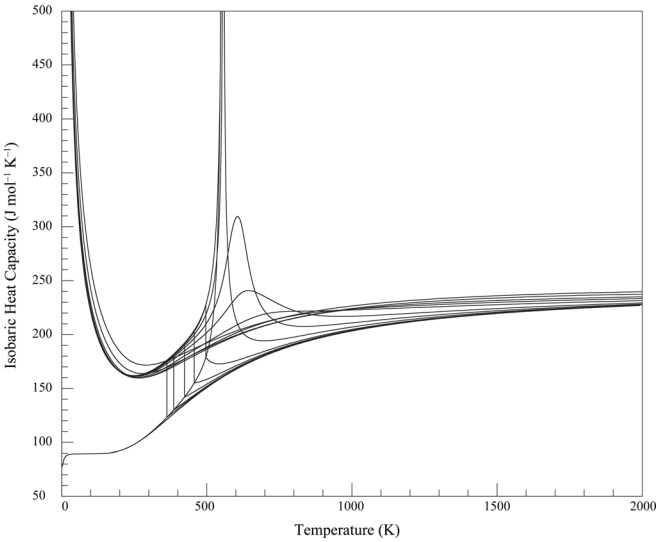

FIG. 8. Isobaric heat capacity c_p versus temperature T diagram. Isobars are shown at pressures of (0, 0.1, 0.2, 0.5, 1, 2, p_c, 10, 20, 50, 100, 200, 500, and 1000) MPa.

limited, and are located only on the saturated-liquid line. Comparisons of experimental data with values calculated from the equation of state are not shown in the form of a diagram. The equation represents most of these data within 0.15%.

4.3. The extrapolation behavior of the equation of state

An equation of state should have reasonable extrapolation behavior, and plots of constant property lines on various thermodynamic coordinates are useful in assessing the behavior of an equation of state. The equation developed in this work was used to plot isochoric heat capacity (Fig. 7), isobaric heat capacity (Fig. 8), sound speed (Fig. 9), density versus temperature (Figs. 10 and 11), pressure versus density (Fig. 12), characteristic (ideal) curves[26,30,31] (Fig. 13), and Gruneisen value versus density (Fig. 14).

Figure 7 shows the isochoric heat capacity versus temperature. There is an upward trend around the critical point, and the value of the isochoric heat capacity rises to a local maximum at the critical point. Because we did not use a nonanalytic form for the equation of state, the calculated heat capacity at the critical point is not correct. Figure 8 is a diagram for the isobaric heat capacity versus temperature. Both figures (Figs. 7 and 8) indicate that the behavior of the equation of state is appropriate within the valid range, and that the extrapolation behavior is reasonable at lower and

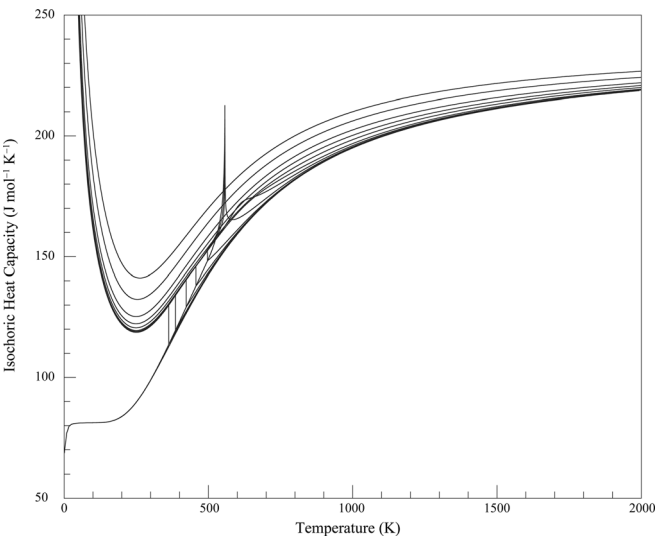

FIG. 7. Isochoric heat capacity c_v versus temperature T diagram. Isobars are shown at pressures of (0, 0.1, 0.2, 0.5, 1, 2, p_c, 10, 20, 50, 100, 200, 500, and 1000) MPa.

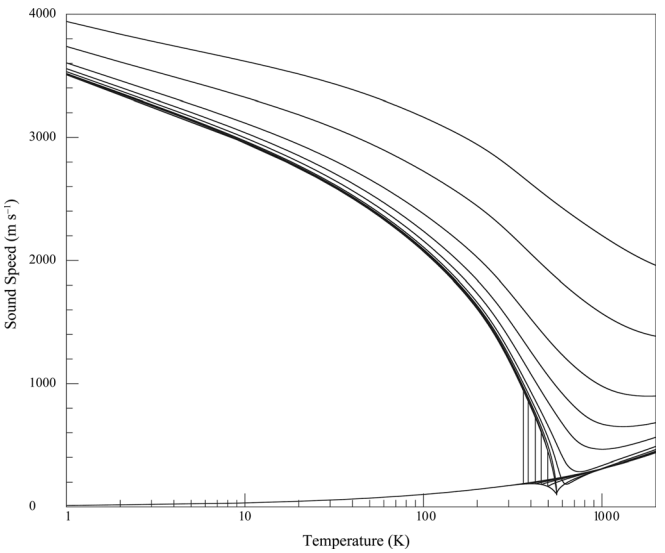

FIG. 9. Speed of sound w versus temperature T diagram. Isobars are shown at pressures of (0, 0.1, 0.2, 0.5, 1, 2, p_c, 10, 20, 50, 100, 200, 500, and 1000) MPa.

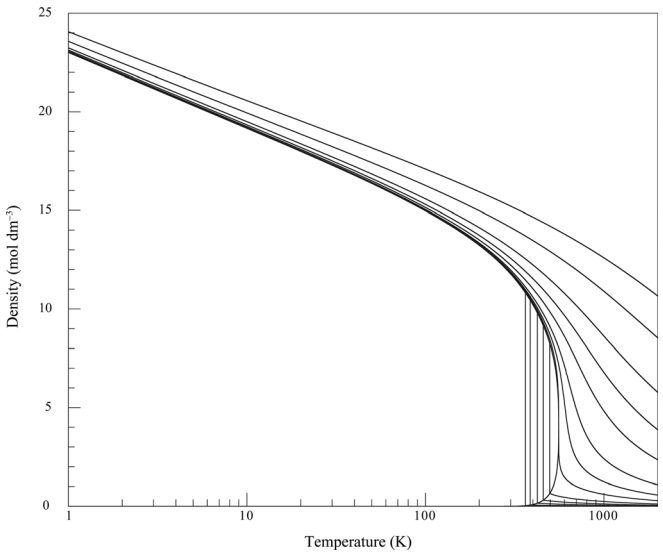

FIG. 10. Density behavior along isobars from very low to high temperatures of the equation of state for dimethyl carbonate. Isobars are shown at pressures of (0, 0.1, 0.2, 0.5, 1, 2, p_c, 10, 20, 50, 100, 200, 500, and 1000) MPa.

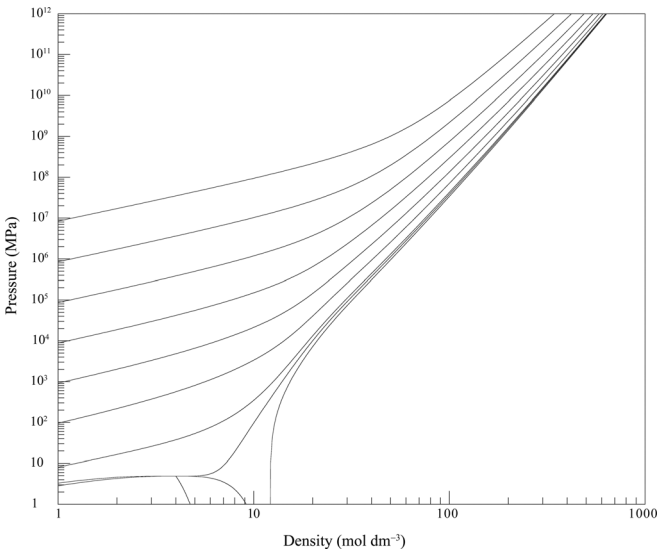

FIG. 12. Isothermal behavior of the equation of state at extreme conditions of temperature T, pressure p, and density ρ. Isotherms are shown at temperatures of (T_{tp}, T_c, 10^3, 10^4, 10^5, 10^6, 10^7, 10^8, and 10^9) K.

higher temperatures and pressures. In addition, Figs. 7 and 8 show that there is a reasonable upward trend in the liquid region at low temperatures below the triple-point temperature,[31] as expected. Figure 9 shows sound speed versus temperature along the saturation lines and along isobars. The figure shows that the saturation line for the liquid is a smooth arc when displayed on a logarithmic scale, and that the extrapolation behavior to high temperatures and pressures is reasonable. As with the isochoric heat capacity, the true nonanalytic behavior of the speed of sound at the critical point cannot be calculated with the equation of state presented here.

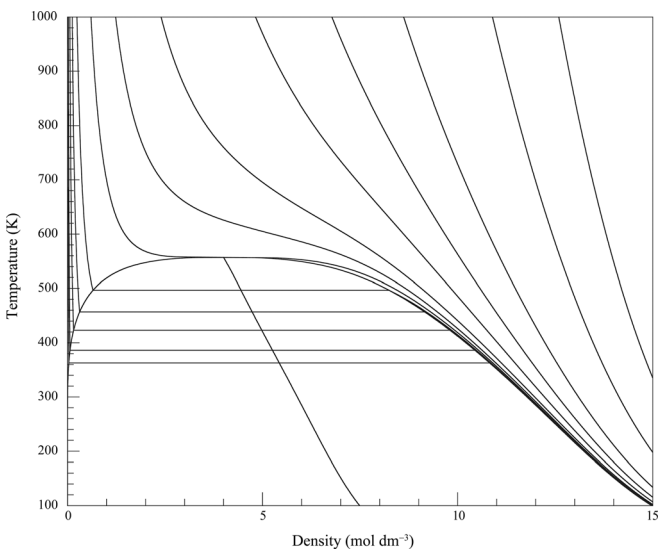

FIG. 11. Density behavior along isobars of the equation of state for dimethyl carbonate. The straight line intersecting the critical point is the rectilinear diameter. Isobars are shown at pressures of (0, 0.1, 0.2, 0.5, 1, 2, p_c, 10, 20, 50, 100, 200, 500, and 1000) MPa.

Figures 10 and 11 show the density behavior along isobars of the equation of state. Figure 10 shows that the liquid isobars are straight on a logarithmic scale down to very low temperature. The rectilinear diameter, which is shown in Fig. 11, has near zero curvature, as it should, up to the critical point. The constraint used in the fit to obtain this effect helps ensure that vapor densities are more reliable.[30] As shown in Fig. 11, the isobars near the critical point are nearly flat, as is typical with all fluids. Further analysis shows that the slope of the critical isobar is positive everywhere.[30]

Figure 12 indicates that the extrapolation behavior to extremely high temperatures, pressures, and densities is reasonable. As explained by Lemmon and Jacobsen,[30] the smooth behavior comes from the term with $t_i = 1$ and $d_i = 5$ (the first term of the residual Helmholtz energy).

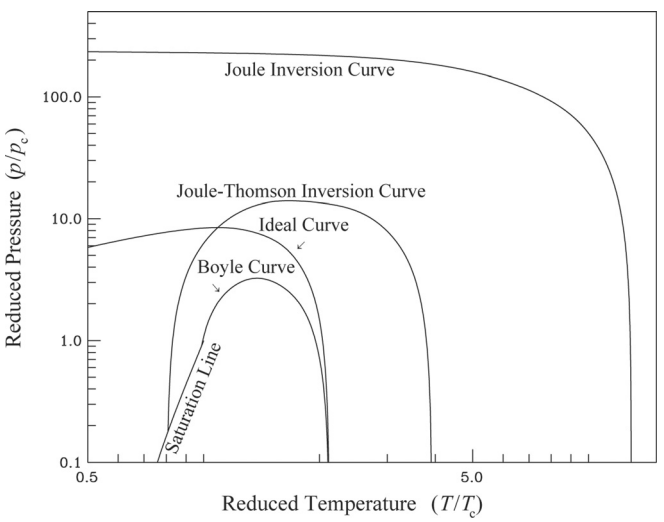

FIG. 13. Characteristic (ideal) curves of the equation of state as a function of reduced temperature T/T_c and reduced pressure p/p_c.

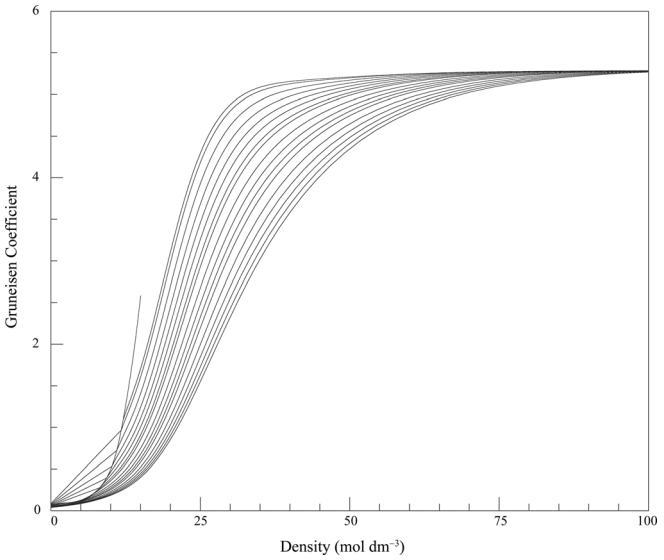

FIG. 14. Gruneisen parameter γ versus density ρ diagram. Isotherms are shown at temperatures of (T_{tp}, 300, 350, 400, 450, 500, T_c, 600, 700, 800, 900, 1000, 1200, 1400, 1600, 1800, and 2000) K.

Figure 13 shows the characteristic (ideal) curves of the equation of state as a function of reduced temperature T/T_c and reduced pressure p/p_c. Figure 13 is used to assess the behavior of the equation in regions without available experimental data.[26,30,31] The characteristic curves include the Boyle curve, the Joule-Thomson inversion curve, the Joule inversion curve, and the ideal curve. The Boyle curve is given by

$$\left(\frac{\partial Z}{\partial v}\right)_T = 0. \tag{12}$$

The Joule-Thomson inversion curve is given by

$$\left(\frac{\partial Z}{\partial T}\right)_p = 0. \tag{13}$$

The Joule inversion curve is given by

$$\left(\frac{\partial Z}{\partial T}\right)_v = 0. \tag{14}$$

The ideal curve is given by

$$Z \equiv \frac{p}{\rho RT} = 1. \tag{15}$$

The Gruneisen parameter γ, which cannot be measured directly, is given by

$$\gamma = v\left(\frac{\partial p}{\partial e}\right)_v = \frac{\alpha_v k_s}{c_p \rho} = \frac{\alpha_v k_T}{c_v \rho}. \tag{16}$$

The Gruneisen parameter is a combination of different properties, and the reasonable behavior of the Gruneisen parameter, shown in Fig. 14, indicates that other properties and the equation of state are more likely to be correct because of the sensitive nature of this property.[34]

Overall, these plots indicate that the equation of state behavior is accurate within the valid range, and that the extrapolation behavior is reasonable at higher and lower temperatures and at higher pressures.

5. Conclusions

The equation of state for dimethyl carbonate, valid from the triple-point temperature (277.06 ± 0.63) K to 600 K with pressures up to 60 MPa, was fitted with the Helmholtz energy as the fundamental property, and temperature and density as the independent variables. The equation is based on experimental $p\rho T$ data, heat capacities, sound speeds, vapor pressures, and saturated-liquid densities. The uncertainties ($k = 2$, indicating a level of confidence of 95%) of the equation of state in density are 0.05% for saturated-liquid states below 350 K, rising to 0.1% in the single phase between 278 K and 400 K at pressures up to 60 MPa. Due to the lack of reliable data outside this region, the estimated uncertainties increase to 0.5% to 1% in the vapor and critical regions. The uncertainties in vapor pressure are 0.6% from 310 K to 400 K, and increase to 1% at higher temperatures and to 2% at lower temperatures due to a lack of experimental data. The uncertainty in isobaric heat capacity and speed of sound in the liquid phase at saturation or atmospheric pressure is 0.5% from 280 K to 335 K. The uncertainties are higher for all properties in the critical region. The extrapolation behavior of the equation of state at low and high temperatures and pressures is reasonable.

Vapor pressures and saturated-liquid densities above 400 K should be further measured to decrease the uncertainty in new equations, along with density measurements in the vapor phase. Additionally, there is a need for further measurements of caloric properties, including heat capacity and sound speed.

6. Acknowledgments

We thank Mostafa Salehi from NIST for his assistance in the literature search. Yong Zhou and Jiangtao Wu acknowledge support from the Foundation for the Author of National Excellent Doctoral Dissertation (Grant 200540) and Fok Ying Tung Education Foundation (Project Number 111060).

7. References

[1]Y. Katrib, G. Deiber, P. Mirabel, S. L. Calve, C. George, A. Mellouki, and G. L. Bras, J. Atmos. Chem. **43**, 151 (2002).
[2]F. K. Wang, J. T. Wu, and Z. G. Liu, Fluid Phase Equilib. **220**, 123 (2004).
[3]Clean Air Act Amendments of 1990, Pub. L. 101-549, 104 Stat. 2399, 1990-11-15 (1990).
[4]M. A. Pacheco and C. L. Marshall, Energy Fuels **11**, 2 (1997).
[5]W. V. Steele, R. D. Chirico, S. E. Knipmeyer, and A. Nguyen, J. Chem. Eng. Data **42**, 1008 (1997).

[6]W. V. Steele, R. D. Chirico, S. E. Knipmeyer, A. Nguyen, and N. K. Smith, J. Chem. Eng. Data **42**, 1037 (1997).
[7]P. Wachter, H. G. Schweiger, F. Wudy, and H. J. Gores, J. Chem. Thermodyn. **40**, 1542 (2008).
[8]M. S. Ding, J. Chem. Eng. Data **49**, 276 (2004).
[9]W. Biltz, W. Fischer, and E. Wunnenberg, Z. Phys. Chem. Abt. A **151**, 13 (1930).
[10]M. Frenkel, R. D. Chirico, V. Diky, C. D. Muzny, A. F. Kazakov, J. W. Magee, I. M. Abdulagatov, and J. W. Kang, *NIST ThermoData Engine*, *NIST Standard Reference Database 103b, Version 5.0* (National Institute of Standards and Technology, Standard Reference Data Program: Gaithersburg, MD, 2010).
[11]L. Lugo, M. J. P. Comunas, E. R. Lopez, and J. Fernandez, Fluid Phase Equilib. **186**, 235 (2001).
[12]M. J. P. Comunas, A. Baylaucq, C. Boned, and J. Fernandez, Int. J. Thermophys. **22**, 749 (2001).
[13]J. Troncoso, D. Bessieres, C. A. Cerdeirina, E. Carballo, and L. Romani, J. Chem. Eng. Data **49**, 923 (2004).
[14]X. Y. Meng, P. J. Zheng, J. T. Wu, and Z. G. Liu, J. Eng. Thermophys. **30**, 26 (2009).
[15]B. Y. Jiang and J. H. Zhang, J. Tianjin Univ. **20**, 53 (1987).
[16]A. Rodriguez, J. Canosa, A. Dominguez, and J. Tojo, Fluid Phase Equilib. **198**, 95 (2002).
[17]S. A. Kozlova, V. N. E. Yanenko, M. Georgieva, S. P. Verevkin, Y. Chernyak, B. Schaffner, and A. Borner, J. Chem. Thermodyn. **40**, 1136 (2008).
[18]J. M. Pardo, C. A. Tovar, C. A. Cerdeirina, E. Carballo, and L. Romania, J. Chem. Thermodyn. **31**, 787 (1999).
[19]J. M. P. Regueiro, Ph.D. thesis, Universidad de Vigo, 1999.
[20]J. M. Pardo, C. A. Tovar, C. A. Cerdeirina, E. Carballo, and L. Romani, Fluid Phase Equilib. **179**, 151 (2001).
[21]J. M. Pardo, D. Gonzalez-Salgado, C. A. Tovar, C. A. Cerdeirina, E. Carballo, and L. Romani, Can. J. Chem. **80**, 370 (2002).
[22]J. M. Pardo, C. A. Tovar, J. Troncoso, E. Carballo, and L. Romani, Thermochim. Acta **433**, 128 (2005).
[23]J. L. Valencia, J. Troncoso, J. Peleteiro, E. Carballo, and L. Romani, Fluid Phase Equilib. **232**, 207 (2005).
[24]F. Comelli, R. Francesconi, A. Bigi, and K. Rubini, J. Chem. Eng. Data **51**, 665 (2006).
[25]F. Comelli, A. Bigi, D. Vitalini, and K. Rubini, J. Chem. Eng. Data **55**, 205 (2010).
[26]R. Span, *Multiparameter Equations of State: An Accurate Source of Thermodynamic Property Data* (Springer, New York, 2000).
[27]R. T. Jacobsen, S. G. Penoncello, and E. W. Lemmon, in *Equations of State for Fluids and Fluid Mixtures*, edited by J. V. Sengers, R. F. Kayser, and C. J. Peters (Elsevier, Amsterdam, 2000), Vol. V, p. 35.
[28]P. J. Mohr, B. N. Taylor, and D. B. Newell, J. Phys. Chem. Ref. Data **37**, 1187 (2008).
[29]R. Span and W. Wagner, Int. J. Thermophys. **18**, 1445 (1997).
[30]E. W. Lemmon and R. T. Jacobsen, J. Phys. Chem. Ref. Data **34**, 69 (2005).
[31]E. W. Lemmon, M. O. McLinden, and W. Wagner, J. Chem. Eng. Data **54**, 3141 (2009).
[32]L. Negadi, A. Blondel, I. Mokbel, A. Ait-Kaci, and J. Jose, Int. Data Ser., Sel. Data Mixtures, Ser. A **21**, 169 (1993).
[33]H. G. Harris, Ph.D. thesis, University of California, 1961.
[34]E. W. Lemmon, V. D. Arp, and D. O. Ortiz-Vega, "The Gruneisen parameter and fluid state equations" (unpublished).
[35]F. Comelli and R. Francesconi, J. Chem. Eng. Data **39**, 560 (1994).
[36]L. Q. Zhang, J. G. Chen, and J. H. Ding, Speciality Petrochemicals **20**, 42 (2003).
[37]Y. H. Shi, H. L. Liu, K. Wang, W. D. Xiao, and Y. Hu, Fluid Phase Equilib. **234**, 1 (2005).
[38]M. Fukano, H. Matsuda, K. Kurihara, and K. Ochi, J. Chem. Eng. Data **51**, 1458 (2006).
[39]H. L. Li, R. J. Zhu, Y. L. Tan, H. F. Xu, and Z. L. Dong, J. Chem. Eng. Data **53**, 2095 (2008).
[40]E. R. Lopez, L. Lugo, M. J. P. Comunas, J. Garcia, and J. Fernandez, J. Chem. Thermodyn. **32**, 743 (2000).
[41]A. Rodriguez, J. Canosa, and J. Tojo, J. Chem. Eng. Data **46**, 1476 (2001).
[42]S. S. Bi, J. T. Wu, Z. G. Liu, and X. Y. Meng, J. Xi'an Jiaotong Univ. **37**, 903 (2003).
[43]E. Romano, J. L. Trenzado, E. Gonzalez, J. S. Matos, L. Segade, and E. Jimenez, Fluid Phase Equilib. **211**, 219 (2003).
[44]A. B. Pereiro, A. Rodriguez, J. Canosa, and J. Tojo, J. Chem. Eng. Data **49**, 1392 (2004).
[45]M. A. Rivas, S. M. Pereira, N. Banerji, and T. P. Iglesias, J. Chem. Thermodyn. **36**, 183 (2004).
[46]J. Tojo, J. Canosa, A. Rodriguez, J. Ortega, and R. Diepp, J. Chem. Eng. Data **49**, 86 (2004).
[47]C. S. Yang, W. Xu, and P. S. Ma, J. Chem. Eng. Data **49**, 1802 (2004).
[48]A. Rodriguez, A. B. Pereiro, J. Canosa, and J. Tojo, J. Chem. Thermodyn. **38**, 505 (2006).
[49]M. A. Iglesias-Otero, J. Troncoso, E. Carballo, and L. Romani, J. Solution Chem. **36**, 1219 (2007).
[50]M. A. Rivas and T. P. Iglesias, J. Chem. Thermodyn. **39**, 1546 (2007).
[51]M. A. Rivas and T. P. Iglesias, J. Chem. Thermodyn. **40**, 1120 (2008).
[52]L. Mosteiro, A. B. Mariano, L. M. Casas, M. M. Pineiro, and J. L. Legido, J. Chem. Eng. Data **54**, 1056 (2009).
[53]P. S. Ma and N. N. Li, J. Tianjin Univ. **38**, 577 (2005).
[54]J. Wisniak, G. Cortez, R. D. Peralta, R. Infante, L. E. Elizalde, T. A. Amaro, O. García, and H. Soto, J. Chem. Thermodyn. **40**, 1671 (2008).